Q-switched waveguide laser based on two-dimensional semiconducting materials: tungsten disulfide and black phosphorous

Yang Tan,[1,*] Zhinan Guo,[2] Linan Ma,[1] Han Zhang,[2,4] Shavkat Akhmadaliev,[3] Shengqiang Zhou,[3] and Feng Chen[1]

[1]*School of Physics, State Key Laboratory of Crystal Materials, Key Laboratory of Particle Physics and Particle Irradiation (Ministry of Education) Shandong University, Jinan 250100, China*
[2]*SZU-NUS Collaborative Innovation Center for Optoelectronic Science and Technology, Key Laboratory of Optoelectronic Devices and Systems of Ministry of Education and Guangdong Province, College of Optoelectronic Engineering, Shenzhen University, Shenzhen 518060, China*
[3]*Helmholtz-Zentrum Dresden-Rossendorf, Institute of Ion Beam and Materials Research, Bautzner Landstrasse 400, 01328 Dresden, Germany*
[4]*hzhang@szu.edu.cn*
[*]*tanyang@sdu.edu.cn*

Abstract: Owing to their unique properties, graphene-like two dimensional semiconducting materials, including Tungsten Disulfide (WS_2) and Black Phosphorous (BP), have attracted increasing interest from basic research to practical applications. Herein, we demonstrated the ultrafast nonlinear saturable absorption response of WS_2 and BP films in the waveguide structure. Through fabricating WS_2 and BP films by evaporating the solutions on glass wafers. Saturable absorber films were attached onto the end-facet of the waveguide, which therefore constitutes a resonant cavity for the waveguide laser. Under a pump laser at 810 nm, we could obtain a stable Q-switched operation in the waveguide structure. This work indicated the significant potential of WS_2 and BP for the ultrafast waveguide laser.

©2016 Optical Society of America

OCIS codes: (230.7380) Waveguides, channeled; (140.3540) Lasers, Q-switched; (130.0130) Integrated optics.

References and links

1. F. Xia, H. Wang, D. Xiao, M. Dubey, and A. Ramasubramaniam, "Two-dimensional material nanophotonics," Nat. Photonics **8**(12), 899–907 (2014).
2. A. V. Kretinin, Y. Cao, J. S. Tu, G. L. Yu, R. Jalil, K. S. Novoselov, S. J. Haigh, A. Gholinia, A. Mishchenko, M. Lozada, T. Georgiou, C. R. Woods, F. Withers, P. Blake, G. Eda, A. Wirsig, C. Hucho, K. Watanabe, T. Taniguchi, A. K. Geim, and R. V. Gorbachev, "Electronic properties of graphene encapsulated with different two-dimensional atomic crystals," Nano Lett. **14**(6), 3270–3276 (2014).
3. T. Roy, M. Tosun, J. S. Kang, A. B. Sachid, S. B. Desai, M. Hettick, C. C. Hu, and A. Javey, "Field-effect transistors built from all two-dimensional material components," ACS Nano **8**(6), 6259–6264 (2014).
4. G. Fiori, F. Bonaccorso, G. Iannaccone, T. Palacios, D. Neumaier, A. Seabaugh, S. K. Banerjee, and L. Colombo, "Electronics based on two-dimensional materials," Nat. Nanotechnol. **9**(10), 768–779 (2014).
5. H. Mu, S. Lin, Z. Wang, S. Xiao, P. Li, Y. Chen, H. Zhang, H. Bao, S. P. Lau, C. Pan, D. Fan, and Q. Bao, "Black Phosphorus–Polymer Composites for Pulsed Lasers," Adv. Opt. Mater. **3**(10), 1447–1453 (2015).
6. Y. Chen, G. Jiang, S. Chen, Z. Guo, X. Yu, C. Zhao, H. Zhang, Q. Bao, S. Wen, D. Tang, and D. Fan, "Mechanically exfoliated black phosphorus as a new saturable absorber for both Q-switching and Mode-locking laser operation," Opt. Express **23**(10), 12823–12833 (2015).
7. J. Kim, S. S. Baik, S. H. Ryu, Y. Sohn, S. Park, B. G. Park, J. Denlinger, Y. Yi, H. J. Choi, and K. S. Kim, "Observation of tunable band gap and anisotropic Dirac semimetal state in black phosphorus," Science **349**(6249), 723–726 (2015).
8. A. Chanana and S. Mahapatra, "First principles study of metal contacts to monolayer black phosphorous," J. Appl. Phys. **116**(20), 204302 (2014).
9. H. O. H. Churchill and P. Jarillo-Herrero, "Two-dimensional crystals: Phosphorus joins the family," Nat. Nanotechnol. **9**(5), 330–331 (2014).
10. X. Hong, J. Kim, S. F. Shi, Y. Zhang, C. Jin, Y. Sun, S. Tongay, J. Wu, Y. Zhang, and F. Wang, "Ultrafast charge transfer in atomically thin MoS_2/WS_2 heterostructures," Nat. Nanotechnol. **9**(9), 682–686 (2014).

#254121 Received 23 Nov 2015; revised 31 Jan 2016; accepted 2 Feb 2016; published 4 Feb 2016

11. Y. Gong, J. Lin, X. Wang, G. Shi, S. Lei, Z. Lin, X. Zou, G. Ye, R. Vajtai, B. I. Yakobson, H. Terrones, M. Terrones, B. K. Tay, J. Lou, S. T. Pantelides, Z. Liu, W. Zhou, and P. M. Ajayan, "Vertical and in-plane heterostructures from WS_2/MoS_2 monolayers," Nat. Mater. **13**(12), 1135–1142 (2014).
12. Y. Chen, G. Jiang, S. Chen, Z. Guo, X. Yu, C. Zhao, H. Zhang, Q. Bao, S. Wen, D. Tang, and D. Fan, "Mechanically exfoliated black phosphorus as a new saturable absorber for both Q-switching and Mode-locking laser operation," Opt. Express **23**(10), 12823–12833 (2015).
13. X. Fu, J. Qian, X. Qiao, P. Tan, and Z. Peng, "Nonlinear saturable absorption of vertically stood WS_2 nanoplates," Opt. Lett. **39**(22), 6450–6453 (2014).
14. S. Zhang, N. Dong, N. McEvoy, M. O'Brien, S. Winters, N. C. Berner, C. Yim, Y. Li, X. Zhang, Z. Chen, L. Zhang, G. S. Duesberg, and J. Wang, "Direct observation of degenerate two-photon absorption and its saturation in WS_2 and MoS_2 monolayer and few-layer films," ACS Nano **9**(7), 7142–7150 (2015).
15. Y. Wang, G. Huang, H. Mu, S. Lin, J. Chen, S. Xiao, Q. Bao, and J. He, "Ultrafast recovery time and broadband saturable absorption properties of black phosphorus suspension," Appl. Phys. Lett. **107**(9), 091905 (2015).
16. B. Zhang, F. Lou, R. Zhao, J. He, J. Li, X. Su, J. Ning, and K. Yang, "Exfoliated layers of black phosphorus as saturable absorber for ultrafast solid-state laser," Opt. Lett. **40**(16), 3691–3694 (2015).
17. C. Grivas, "Optically pumped planar waveguide lasers, Part I: Fundamentals and fabrication techniques," Prog. Quantum Electron. **35**(6), 159–239 (2011).
18. F. Chen and J. R. Vázquez de Aldana, "Optical waveguides in crystalline dielectric materials produced by femtosecond - laser micromachining," Laser Photonics Rev. **8**(2), 251–275 (2014).
19. F. Chen, "Micro - and submicrometric waveguiding structures in optical crystals produced by ion beams for photonic applications," Laser Photonics Rev. **6**(5), 622–640 (2012).
20. Y. Tan, Q. Luan, F. Liu, F. Chen, and J. R. Vázquez de Aldana, "Q-switched pulse laser generation from double-cladding Nd:YAG ceramics waveguides," Opt. Express **21**(16), 18963–18968 (2013).
21. G. Salamu, F. Jipa, M. Zamfirescu, and N. Pavel, "Laser emission from diode-pumped Nd:YAG ceramic waveguide lasers realized by direct femtosecond-laser writing technique," Opt. Express **22**(5), 5177–5182 (2014).
22. N. Pavel, G. Salamu, F. Jipa, and M. Zamfirescu, "Diode-laser pumping into the emitting level for efficient lasing of depressed cladding waveguides realized in $Nd:YVO_4$ by the direct femtosecond-laser writing technique," Opt. Express **22**(19), 23057–23065 (2014).
23. Y. Tan, H. Zhang, C. Zhao, S. Akhmadaliev, S. Zhou, and F. Chen, "Bi_2Se_3 Q-switched Nd:YAG ceramic waveguide laser," Opt. Lett. **40**(4), 637–640 (2015).
24. Y. Tan, F. Chen, D. Jaque, W. L. Gao, H. J. Zhang, J. G. Solé, and H. J. Ma, "Ion-implanted optical-stripe waveguides in neodymium-doped calcium barium niobate crystals," Opt. Lett. **34**(9), 1438–1440 (2009).
25. A. Choudhary, S. J. Beecher, S. Dhingra, B. D'Urso, T. L. Parsonage, J. A. Grant-Jacob, P. Hua, J. I. Mackenzie, R. W. Eason, and D. P. Shepherd, "456-mW graphene Q-switched Yb:yttria waveguide laser by evanescent-field interaction," Opt. Lett. **40**(9), 1912–1915 (2015).
26. S. Y. Choi, T. Calmano, M. H. Kim, D. I. Yeom, C. Kränkel, G. Huber, and F. Rotermund, "Q-switched operation of a femtosecond-laser-inscribed Yb:YAG channel waveguide laser using carbon nanotubes," Opt. Express **23**(6), 7999–8005 (2015).
27. J. W. Kim, S. Y. Choi, S. Aravazhi, M. Pollnau, U. Griebner, V. Petrov, S. Bae, K. J. Ahn, D. Yeom, and F. Rotermund, "Graphene Q-switched Yb:KYW planar waveguide laser," AIP Adv. **5**(1), 017110 (2015).
28. A. Choudhary, S. Dhingra, B. D'Urso, T. L. Parsonage, K. A. Sloyan, R. W. Eason, and D. P. Shepherd, "Q-switched operation of a pulsed-laser-deposited $Yb:Y_2O_3$ waveguide using graphene as a saturable absorber," Opt. Lett. **39**(15), 4325–4328 (2014).
29. Y. Tan, S. Akhmadaliev, S. Zhou, S. Sun, and F. Chen, "Guided continuous-wave and graphene-based Q-switched lasers in carbon ion irradiated Nd:YAG ceramic channel waveguide," Opt. Express **22**(3), 3572–3577 (2014).
30. Q. L. Bao, H. Zhang, Y. Wang, Z. H. Ni, Y. L. Yan, Z. X. Shen, K. P. Loh, and D. Y. Tang, "Atomic-layer graphene as a saturable absorber for ultrafast pulsed lasers," Adv. Funct. Mater. **19**(19), 3077–3083 (2009).
31. D. Mao, Y. Wang, C. Ma, L. Han, B. Jiang, X. Gan, S. Hua, W. Zhang, T. Mei, and J. Zhao, "WS_2 mode-locked ultrafast fiber laser," Sci. Rep. **5**, 7965 (2015).
32. E. Lallier, J. P. Pocholle, M. Papuchon, M. P. De Micheli, M. J. Li, Q. He, D. B. Ostrowsky, C. Grezes-Besset, and E. Pelletier, "$Nd:MgO:LiNbO_3$ channel waveguide laser devices," IEEE J. Quantum Electron. **27**(3), 618–625 (1991).
33. X. Zhang, S. Zhao, Q. Wang, Q. Zhang, L. Sun, and S. Zhang, "Optimization of Cr^{4+}-doped saturable-absorber Q-switched lasers," IEEE J. Quantum Electron. **33**(12), 2286–2294 (1997).
34. Y. F. Chen, Y. P. Lan, H. L. Chang, and J. Quan, "Analytical model for design criteria of passively Q-switched lasers," IEEE J. Quantum Electron. **37**(3), 462–468 (2001).
35. J. J. Zayhowski and P. L. Kelley, "Optimization of Q-switched lasers," IEEE J. Quantum Electron. **27**(9), 2220–2225 (1991).
36. G. J. Spühler, R. Paschotta, R. Fluck, B. Braun, M. Moser, G. Zhang, E. Gini, and U. Keller, "Experimentally confirmed design guidelines for passively Q-switched microchip lasers using semiconductor saturable absorbers," J. Opt. Soc. Am. B **16**(6), 376–388 (1999).

#254121 Received 23 Nov 2015; revised 31 Jan 2016; accepted 2 Feb 2016; published 4 Feb 2016
(C) 2016 OSA

1. Introduction

Two-dimensional (2D) material, including graphene and graphen-like materials, is a booming family of nanomaterials with outstanding physical and chemical properties [1–4]. The investigation of novel 2D materials opens up a new play-ground with unprecedented chances for testing and realizing conceptually new electronic and optoelectronic devices. Recently, Black Phosphorous (BP) [5] and Tungsten Disulfide (WS_2) [6] have joined in the family of the 2D material and attracted intense interests in both electronics and optics, because of their unique properties that may compensate the disadvantges of graphene [7–11].

Similar as graphene, BP is comprised by only the elemental phosphorus and can be easily peeled off by mechanical exfoliation [12]. As the most thermo-dynamically stable allotrope of phosphorus, BP has a layer-dependent direct band-gap changing from 0.35 eV (bulk) to 2 eV (monolayer layer), which makes BP capable of filling the blank space between semi-metallic graphene and wide band-gap transition-metal dichalcogenides. Analogous to MoS_2, WS_2 is another layered transition metal dichalcogenide. Each atomic layer of WS_2 consists of a layer tungsten sandwiched by two layers of sulphur. The indirect band gap of bulk WS_2 is ~1.3 eV while the direct band gap of its monolayer can increase up to 2.1 eV. In optics, it has been demonstrated that BP and WS_2 have the saturable absorption and the broadband nonlinear optics response. It is natural to employ BP and WS_2 as a saturable absorber for Q-switched pulse laser emission [13–16]. Until now, the application in the fiber and bulk laser system has been reported. However there is no report for the applicaiton of BP and WS_2 in the waveguide laser until now.

Waveguide laser is a subminiature laser source, in which the waveguide structure works as the gain medium [17–19]. A few wellknown techniques have been applied for the waveguide fabrication in high-efficiency gain medium (i.e., the rare earth doped crystal and ceramics), including femtosecond laser writing [20–22], implantation [23] and swift ion irradiation. Different from the bulk and fiber laser system, the cavity mode-volume of the waveguide laser is much smaller and is directly fabricated in the active host. Besides, the length of the waveguide laser is much smaller than the fiber and bulk laser.

According to these differences, there are several advantages of the waveguide laser in the Q-switched pulse laser emission. At first, smaller volume in waveguide allows for much higher intensity density under the same power. Hence the nonlinear optical response of the 2D material can be observed in the waveguide even at the low power. Second, shorter length of the resonant cavity reduces the cavity round-trip time. And the pulse duration of the Q-switched laser can reach a nanosecond order of magnitude even with the low modulation depth less than 1% [24–28].

In this work, performances of BP and WS_2 films in the waveguide were disscussed in details. BP and WS_2 were compressed onto the endfacet of the neodymium doped yttrium aluminum garnet ceramics (Nd:YAG ceramic) waveguide, respectively, as the saturable absorber. Under the pumping laser of 810 nm, the pulse waveguide laser was observed at the wavelength of 1064 nm. And pulse durations was 55 ns (modulated by BP) and 24 ns (modulated by WS_2), respectively, corresponding to the modulation depth of 0.8% (modulated by BP) and 1.8% (modulated by WS_2). Different performances of the output waveguide laser were demenstrated to be induced by diverse saturable absorption properties of BP and WS_2 films. This work confirmed the potential of BP and WS_2 as excellent saturable absorbers for the Q-switched waveguide laser generation.

2. Experiments

2.1. BP and WS_2

Few layers BP and WS_2 films were fabricated by the liquid-phase exfoliation technique which has been proved to be an effective way to produce two-dimensional nano-materials, including graphene, hBN, and TMDs. In experiments, the bulk material (purity 99.998%) was exfoliated and dispersed into N-methylpyrrolidone (NMP) solvent and ultra-sonicated for 4 hours. Due to the breaking down of the inter-layer van der Waals bonding, nanoflakes were formed into

#254121 Received 23 Nov 2015; revised 31 Jan 2016; accepted 2 Feb 2016; published 4 Feb 2016
(C) 2016 OSA

the solution. The large number of thick flackes was removed by centrifuging at a speed of 1500 rpm for 45 minutes. The few-layers BP or WS_2 were transferred from the dispersion to the ethanol. Then the BP or WS_2 liquid was drop-casted onto two silica wafers, respectively, forming saturable absorber mirrors (SAM). Figures 1(a) and 1(b) were images of WS_2 and BP SAMs. Insets of Figs. 1(a) and (b) are the solution of WS_2 (purchase from XFnano.co) and BP, respectively. The Raman spectra of SAMs were displayed in Figs. 1(c) and 1(d) indicating BP and WS_2 films have been well deposited onto wafers.

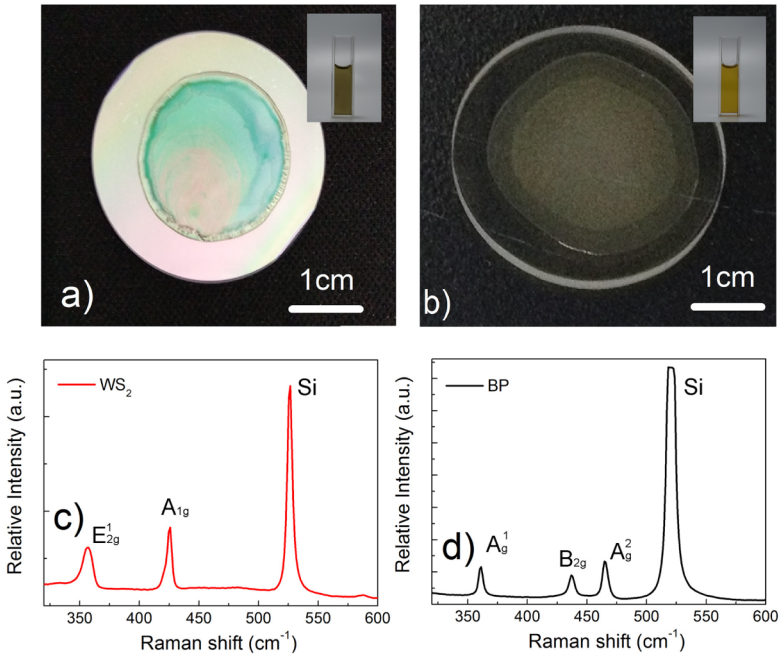

Fig. 1. Images of WS_2 (a) and BP (b) SAMs. Insets of (a) and (b) are solutions of WS_2 and BP, respectively. Measured Raman spectrum of WS_2 (c) and BP (d) film.

2.2. Nd:YAG ceramic waveguide fabrication

The Nd:YAG ceramic doped by 2 at.% Nd^{3+} ion was cut into dimensions of 2 × 10 × 7 mm^3 with all facets optically polished. Using a 3 MV tandem accelerator, the carbon ions with energy of 15 MeV and fluence of 2×10^{14} ions/cm^2 were irradiated onto one biggest facet of the Nd:YAG ceramic. During the irradiation, a mask with open slits (20 μm width and 10 mm length) was put onto the surface of Nd:YAG ceramic. Through the selection of the mask, channel waveguides with the length of 8 mm and width of 20 μm width were formed on the Nd:YAG ceramic. After the irradiation, the Nd:YAG ceramic waveguide was annealed at 180 °C for 1 hour and the propagation loss of the waveguide was reduced to 0.5 dB/cm. Detailed information of the Nd:YAG ceramic waveguide has been reported in [29], Tan et al….

2.3. Experiment for the waveguide laser

Figure 2(a) shows the experimental setup for the laser emission based on the Nd:YAG ceramic waveguide. A mirror (M1) with high reflectivity at 1064 nm was coated onto the input facet of the waveguide as the input mirror. While a silica wafer was used as the output mirror (M2) with the reflectivity of 20% and put onto the output facet. A continuous wave (CW) laser at 810 nm from a Ti:sapphire laser was utilized as the pumping source. Through a Lens (focal length of 20 mm), the pumping laser was coupled into the waveguide and the output light was collected by a long work distance microscope objective (MO).

#254121 Received 23 Nov 2015; revised 31 Jan 2016; accepted 2 Feb 2016; published 4 Feb 2016
(C) 2016 OSA

3. Results and discussion

3.1. CW waveguide laser

Utilizing Nd:YAG ceramic waveguide as the gain medium, the waveguide laser was excited following the experimental setup in Fig. 2(a). With the pumping laser at 810 nm, the stable waveguide laser emission was obtained in the CW regime and the wavelength of the output laser was 1064 nm [Fig. 2(b)]. The fluctuation of the output power was less than 5%. Figure 2(c) shows the power of the output laser as a function of the pumping power. The slope efficiency and the threshold of the output laser were 36% and 50 mW, respectively. The measured near-field intensity distribution of the output laser was also shown in the inset of Fig. 2(c).

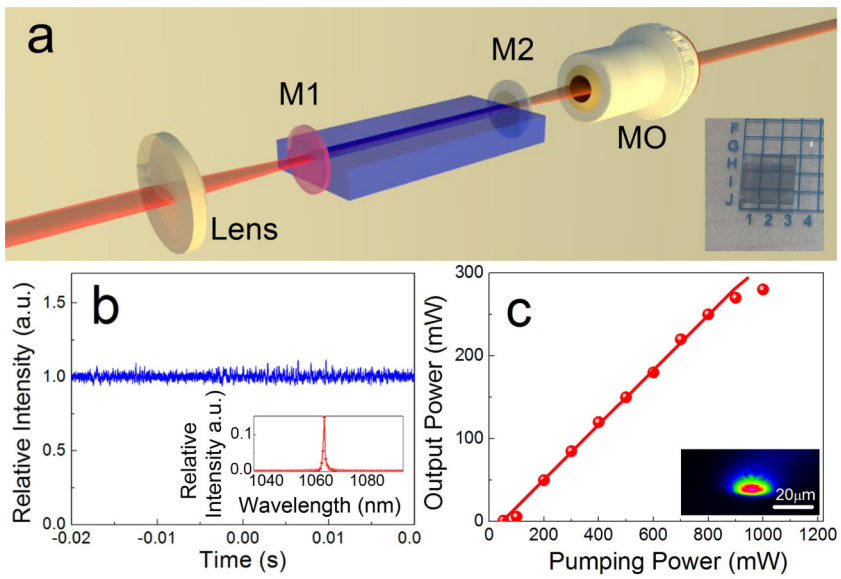

Fig. 2. (a) Schematic plot of the experimental setup for the waveguide laser. The inset is the image of the Nd:YAG ceramic waveguide. (b) The variation of the output laser vs. time under the pump power of 1.08 W at 810 nm. The inset is the emission spectrum at 1064 nm. (c) The output power as a function of the launched pumping power. Inset is the measured near-field modal profile of the emitted laser from the waveguide.

3.2. Q-switched waveguide laser modulated by WS_2

The nonlinear saturable absorption of the prepared WS_2 film was investigated by the z-scan technology. A picosecond laser was used as the probe light source, which has the pulse duration of 22 ps at the wavelength of 1064 nm. The probe light was focused by a lens and vertically irradiated onto the WS_2 film. The variation of the optical intensity on the WS_2 was changed by moving the film to the focal point of the lens. Increasing the optical intensity from 0.1 MW/cm^2 to 600 MW/cm^2, the transmission of the WS_2 film was recorded and depicted in Fig. 3(a). Obviously, the transmission was increased along with the probe light intensity, which demonstrates the saturable absorption of the WS_2 film. For the saturable absorption, the measured nonlinear transmission can be fitted by equations below [30]:

$$\alpha(I) = \alpha_{NS} + \frac{\alpha_s}{1 + \frac{I}{I_s}} \tag{1}$$

$$T(I) = e^{\alpha(I)} \tag{2}$$

#254121 Received 23 Nov 2015; revised 31 Jan 2016; accepted 2 Feb 2016; published 4 Feb 2016
(C) 2016 OSA

where T is the transmission, α is the absorption coefficient, I_s is the saturable intensity and α_s and α_{NS} are saturable and nonsaturable absorption components. The fitted saturable intensity (modulation depth) of the WS_2 film was 35.19 MW/cm^2 (6.5%). This value has the same magnitude of the previous reports [31]. The linear absorption of the WS_2 was also measured to be 3.1 dB under the low intensity (<0.1MW/cm^2) of the excitation light at the wavelength of 1064 nm.

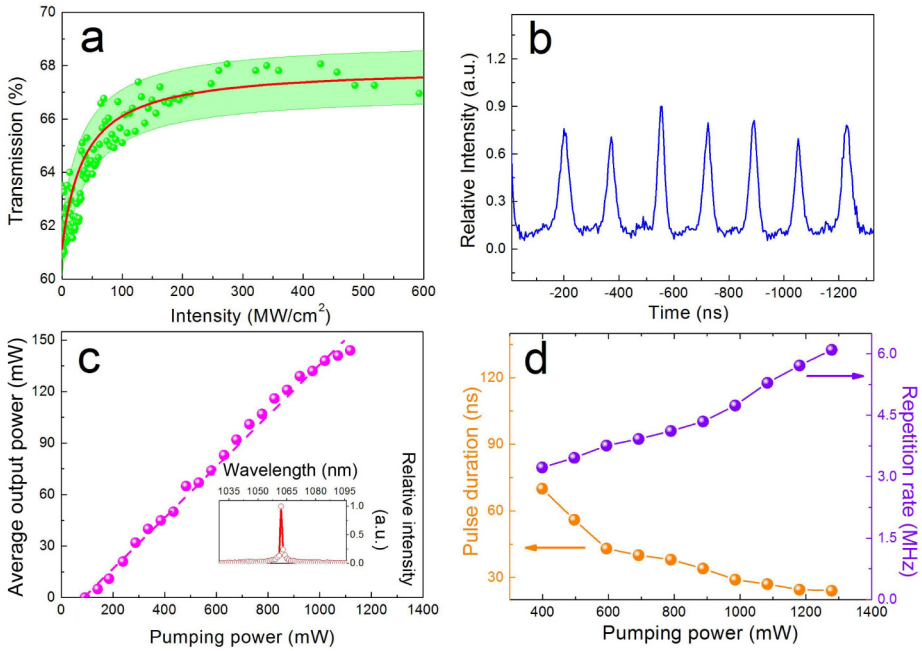

Fig. 3. (a) The nonlinear transmission of the WS_2 film. The green range is the error band. Pulse trains (b), average output power (c), repetition rate and pulse duration (d) of the Q-switched pulse waveguide laser modulated by the WS_2 film. The inset of (c) is the spectrum of the output laser.

The WS_2 film was used as SAM for the Q-switched pulse waveguide laser emission. Following the experimental setup in Fig. 2(a), the WS_2 film replaced M2 as the output mirror. Pumped by a CW laser at 810 nm, the pulse train was obtained [Fig. 3(b)] and the spectrum of the output laser was observed at the wavelength of 1064 nm [inset of Fig. 3(c)]. The maximum output power was 144 mW corresponding to the slope efficiency of 14.4%. The threshold of the pumping power was 90 mW. Please note, the threshold of the waveguide laser was increased for 1.8 times after the replacement of the WS_2 film, which can be attributed to the loss induced by the WS_2 film. In four level system, the laser threshold with M2 (P^{M2}_{th}) or WS_2 (P^{WS2}_{th}) can be expressed as [32]

$$P_{th}^{M2 or WS_2} = \frac{hc}{\lambda_p}\frac{1}{\eta\sigma_e\tau}\frac{\delta^{M2 or WS_2}}{2} \tag{3}$$

$$\delta^{M2} = 2\alpha L - \ln[(1-T_1)\times(1-T_2)] \tag{4}$$

$$\delta^{WS_2} = 2\alpha L + 2\alpha^{WS_2} - \ln[(1-T_1)\times(1-T_2)] \tag{5}$$

where δ^{M2} and δ^{WS2} is the round-trip cavity loss with M2 and WS_2 respectively, h is the Planck's constant, c is the light velocity in the vacuum, λ_p is the wavelength of the pump beam, σ_e is the stimulated emission cross section, τ is the fluorescence lifetime, η is the fraction of absorbed photons that contribute to the population of the $^4F_{3/2}$ metastable state.

#254121 Received 23 Nov 2015; revised 31 Jan 2016; accepted 2 Feb 2016; published 4 Feb 2016
(C) 2016 OSA

Before and after the replacement of WS_2, only the parameter δ was changed. According the measured CW threshold and δ_{M2} (round-trip cavity loss in the CW regime), the cavity loss induced by the WS_2 film was calculated to be 3.7 dB, which has a good agreement with the measured linear absorption of WS_2.

Figure 3(d) shows the variation of the pulse duration and the repetition rate with the pumping power. The repetition rate was increased from 3.23 MHz to 6.10 MHz with an approximate linear variation. The pulse duration of the output laser was 70 ns and rapid decreasing under the low pumping power. Increasing the pumping power, the pulse duration was stable at 24 ns. Please note, the modulation depth was changed along with the laser intensity in the waveguide. As the intensity of the excitation laser was much lower than the threshold of the saturable absorber. According to the second threshold criterion [33, 34], it is not an optimal condition for the passive Q-switched laser. Thus, there are variations of the pulse duration and pulse energy along with the pumping power.

3.3. Q-switched waveguide laser modulated by BP

The nonlinear optical property of the BP film was also measured by the z-scan technology under the same treatment with the WS_2 film. Figure 4(a) shows the nonlinear transmission of the BP film measured at the wavelength of 1064 nm. The intensity of the detecting light was increased from 0.1 MW/cm^2 to 1200 MW/cm^2. Along with the intensity increasing, the transmission was increased, which demonstrates the saturable absorption of the BP film. Fitted by Eq. (2), the saturable intensity was 261 MW/cm^2 and the modulation depth was 25%. The linear absorption was measured to be 4.2 dB at the wavelength of 1064 nm.

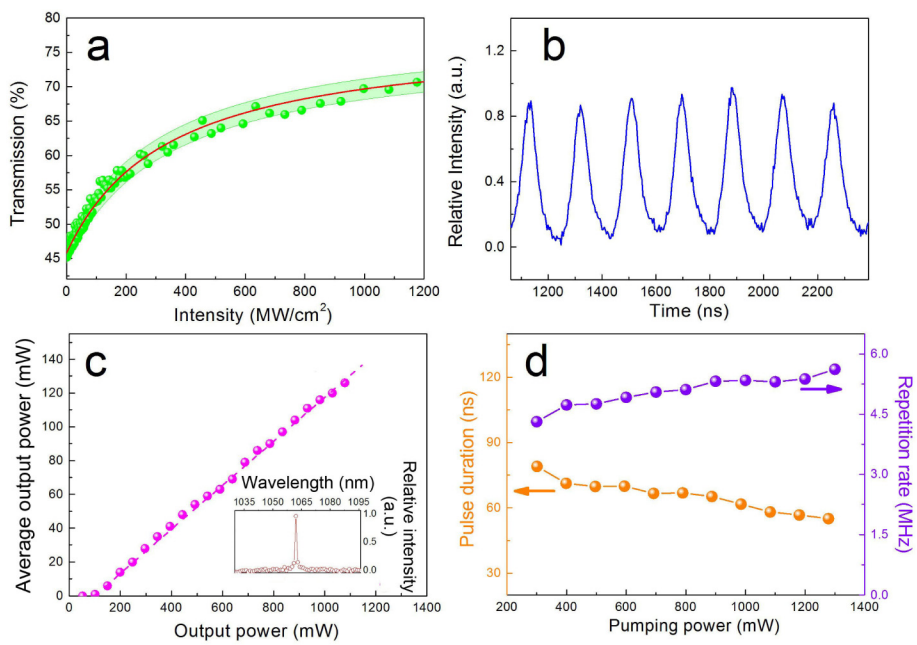

Fig. 4. (a) The nonlinear transmission of the BP film. Green range is the error band. Pulse trains (b), average output power (c), repetition rate and pulse duration (d) of the Q-switched pulse waveguide laser modulated by the BP film. The inset of (c) is the spectrum of the output laser.

Utilizing the BP film as SAM, the pulse laser emission was also obtained from the waveguide. Figure 4(b) shows the pulse train under the pumping power of 1.08 W at the wavelength of 810 nm. The spectrum of the output laser beam was shown in the inset of Fig. 4(c) at a pumping power of 400 mW, which was centered at a wavelength of 1064 nm. The average output power was displayed in Fig. 4(d). The maximum output power was 126 mW

#254121 Received 23 Nov 2015; revised 31 Jan 2016; accepted 2 Feb 2016; published 4 Feb 2016
(C) 2016 OSA

and threshold was 100 mW corresponding to the slope efficiency of 12.9%. Based on the measured laser threshold, the linear absorption of the BP film was calculated to 4.6 dB, which also has a good agreement with the measured linear absorption (4.2 dB). The performance of the emitted pulse laser was demonstrated in Fig. 4(d). With the increasing of the pumping power, the pulse duration was decreased from 79 ns to 55 ns. Meanwhile, the repetition rate could be tuned between 4.3 MHz and 5.6 MHz.

3.4. Comparison of the Q-switched pulse waveguide laser modulated by BP and WS_2 films

According to the minimum pulse duration in Fig. 3(d) and Fig. 4(d), the modulation depth of the WS_2 and BP were calculated by the equation below [35, 36].

$$\tau_p = \frac{3.52T_R}{\Delta R} \tag{6}$$

where ΔR is the modulation depth, τ_p is the pulse duration, and T_R is the cavity round-trip time. Figure 5(a) shows calculated modulation depths of BP and WS_2, respectively. At the low pumping power, the modulation depth was ~0.6% for both BP and WS_2 films. Under the pumping power of 1300 mW, the modulation depth of WS_2 and BP were 1.8% and 0.8%. The modulation depth of WS_2 was 2.3 times larger than that of BP. Since the saturable intensity of the WS_2 is much lower than BP. Hence WS_2 is easier to get a higher modulation depth under the same pumping power. The peak power of the output pulse laser was displayed in Fig. 5(b). Modulated by WS_2 film, the peak power was increased from 0.1 W to 1 W and reached a saturable value with the pumping power above 1.2 W. While, the one modulated by BP stayed at a relative low level. And the value of the peak power was slowly increased from 0.18 W to 0.4 W.

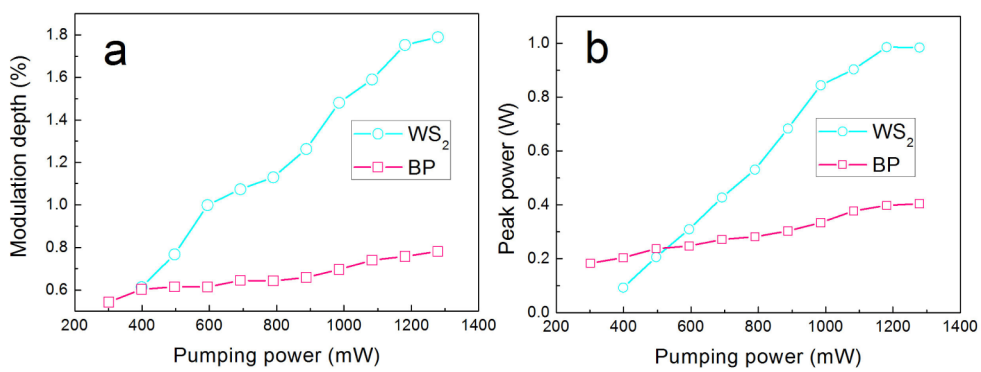

Fig. 5. The modulation depth (a) and the peak power (b) of the output pulse laser as a function of the pumping power modulated by WS_2(circles) and BP (squares), respectively.

4. Conclusions

In conclusion, the ultrafast saturable absorption property of WS_2 and BP films had been investigated in the waveguide structure. Films were utilized as the saturable absorber and integrated with the Nd:YAG ceramic waveguide structure for the Q-switched laser emission. Nanosecond laser was obtained from the waveguide modulated by WS_2 and BP, respectively. This work suggests the WS_2 and BP can be developed as promising nonlinear optical materials for ultrafast photonic application as the saturable absorber for Q-switcher or mode-locker.

Acknowledgments

This research work is supported by the following funding programs: National Natural Science Foundation of China (Grant No. 11535008, by F. C. and Grant Nos. 61435010, 61435010 and

61222505 by H. Z.), Young Scholars Program of Shandong University (Grant No. 2015WLJH20 by Y. T.) I and Helmholtz Association (VH-NG-713 by S. Z.). Ion irradiation has been performed at the Ion Beam Center at the Helmholtz-Zentrum Dresden – Rossendorf.

#254121 Received 23 Nov 2015; revised 31 Jan 2016; accepted 2 Feb 2016; published 4 Feb 2016
(C) 2016 OSA

218.17.207.81 {ts '2016-09-21 01:24:33'}